Manipulating metal-oxide nanowires using counter-propagating optical line tweezers

Astrid van der Horst[1,3,*], **Andrew I. Campbell**[1,*], **Lambert K. van Vugt**[2], **Daniël A. M. Vanmaekelbergh**[2], **Marileen Dogterom**[3], **and Alfons van Blaaderen**[1]

[1]*Soft Condensed Matter, Debye Institute, Utrecht University, Princetonplein 5, 3584 CC Utrecht, The Netherlands*

[2]*Condensed Matter and Interfaces, Debye Institute, Utrecht University, Princetonplein 5, 3584 CC Utrecht, The Netherlands*

[3]*FOM Institute for Atomic and Molecular Physics AMOLF, Kruislaan 407, 1098 SJ Amsterdam, The Netherlands*

[*]These authors contributed equally to this work

astridv@sfu.ca

andrew.campbell@manchester.ac.uk

A.vanBlaaderen@phys.uu.nl

http:www.colloid.nl

Abstract: Semiconducting nanowires, such as ZnO and Si, are used in the fields of nanophotonics and nanoelectronics. Optical tweezers offer the promise of flexible positional control of such particles in a liquid, but so far this has been limited to either manipulation close to the surface, or to axial trapping of nanowires. We show the three-dimensional trapping of ZnO and silica-coated Si nanowires in counter-propagating line tweezers, and demonstrate translational and rotational in-plane manipulation, away from the surfaces. The high-refractive index particles investigated — ZnO wires ($n \sim 1.9$) with varying lengths up to $20\,\mu$m and 6-μm-long silica-coated Si wires ($n = 3.6$) — could not be trapped in single-beam line traps. Opposite surface charges are used to fix the nanowires to a surface. Full translational and in-plane rotational control of semiconducting nanowires expands the possibilities to position individual wires in complex geometries significantly.

© 2007 Optical Society of America

OCIS codes: (140.7010) Trapping; (170.4520) Optical confinement and manipulation. (160.4670) Optical materials.

References and links

1. L. K. van Vugt, S. Rühle, and D. Vanmaekelbergh, "Phase-Correlated Nondirectional Laser Emission from the End Facets of a ZnO Nanowire," Nano Lett. **6**, 2707–2711 (2006).
2. Y. Cui and C. M. Lieber, "Functional Nanoscale Electronic Devices Assembled Using Silicon Nanowire Building Blocks," Science **291**, 851–853 (2001).
3. D. J. Sirbuly, M. Law, H. Yan, and P. Yang, "Semiconductor Nanowires for Subwavelength Photonics Integration," J. Phys. Chem. B **109**, 15190–15213 (2005).
4. D. J. Sirbuly, M. Law, P. Pauzauskie, H. Yan, A. V. Maslov, K. Knutsen, C.-Z. Ning, R. J. Saykally, and P. Yang, "Optical routing and sensing with nanowire assemblies," Proc. Natl. Acad. Sci. USA **102**, 7800–7805 (2005).

5. P. A. Smith, C. D. Nordquist, T. N. Jackson, T. S. Mayer, B. R. Martin, J. Mbindyo, and T. E. Mallouk, "Electric-field assisted assembly and alignment of metallic nanowires," Appl. Phys. Lett. **77**, 1399–1401 (2000).
6. B. Messer, J. H. Song, and P. Yang, "Microchannel Networks for Nanowire Patterning," J. Am. Chem. Soc. **122**, 10232–10233 (2000).
7. T. Yu, F.-C. Cheong, and C.-H. Sow, "The manipulation and assembly of CuO nanorods with line optical tweezers," Nanotechnology **15**, 1732–1736 (2004).
8. R. Agarwal, K. Ladavac, Y. Roichman, G. Yu, C. M. Lieber, and D. G. Grier, "Manipulation and assembly of nanowires with holographic optical traps," Opt. Express **13**, 8906–8912 (2005).
9. P. J. Pauzauskie, A. Radenovic, E. Trepagnier, H. Shroff, P. Yang, and J. Liphardt, "Optical trapping and integration of semiconductor nanowire assemblies in water," Nat. Materials **5**, 97–101 (2006).
10. A. Ashkin, J. M. Dziedzic, J. E. Bjorkholm, and S. Chu, "Observation of a single-beam gradient force optical trap for dielectric particles," Opt. Lett. **11**, 288–290 (1986).
11. A. Ashkin, "Acceleration and trapping of particles by radiation pressure," Phys. Rev. Lett. **24**, 156–159 (1970).
12. S. B. Smith, Y. Cui, and C. Bustamante, "Overstretching B-DNA: The Elastic Response of Individual Double-Stranded and Single-Stranded DNA Molecules," Science **271**, 795–799 (1996).
13. D. L. J. Vossen, A. van der Horst, M. Dogterom, and A. van Blaaderen, "Optical tweezers and confocal microscopy for simultaneous three-dimensional manipulation and imaging in concentrated colloidal dispersions," Rev. Sci. Instrum. **75**, 2960–2970 (2004).
14. K. Visscher, G. J. Brakenhoff, and J. J. Krol, "Micromanipulation by "Multiple" Optical Traps Created by a Single Fast Scanning Trap Integrated With the Bilateral Confocal Scanning Laser Microscope," Cytometry **14**, 105–114 (1993).
15. R. Prasanth, L. K. van Vugt, D. A. M. Vanmaekelbergh, and H. C. Gerritsen, "Resonance enhancement of optical second harmonic generation in a ZnO nanowire," Appl. Phys. Lett. **88**, 181501 (2006).
16. M. H. Huang, Y. Wu, H. Feick, N. Tran, E. Weber, and P. Yang, "Catalytic Growth of Zinc Oxide Nanowires by Vapor Transport," Adv. Mater. **13**, 113–116 (2001).
17. C. M. van Kats, P. M. Johnson, J. E. A. M. van den Meerakker, and A. van Blaaderen, "Synthesis of Monodisperse High-Aspect-Ratio Colloidal Silicon and Silica Rods," Langmuir **20**, 11201–11207 (2004).
18. J. P. Hoogenboom, D. L. J. Vossen, C. Faivre-Moskalenko, M. Dogterom, and A. van Blaaderen, "Patterning surfaces with colloidal particles using optical tweezers," Appl. Phys. Lett. **80**, 4828–4830 (2002).
19. K. D. Bonin, B. Kourmanov, and T. G. Walker, "Light torque nanocontrol, nanomotors and nanorockers," Opt. Express **10**, 984–989 (2002).
20. A. I. Bishop, T. A. Nieminen, N. R. Heckenberg, and H. Rubinsztein-Dunlop, "Optical application and measurement of torque on microparticles of isotropic nonabsorbing material," Phys. Rev. A **68**, 033802 (2003).
21. A. Rohrbach, "Stiffness of Optical Traps: Quantitative Agreement between Experiment and Electromagnetic Theory," Phys. Rev. Lett. **95**, 168102 (2005).

1. Introduction

Semiconducting nanowires, with their efficient and polarized light emission (luminescence), subwavelength waveguiding, and lasing [1], are useful as building blocks in nanoscale electronics [2] or photonic devices [3, 4]. To assemble these building blocks into functional circuits, specific positioning of nanowires is necessary. There are several techniques proposed for manipulation of nanowires and nanorods, such as electric fields [5], micromanipulators [3], and (micro-)fluidics [6].

Recently, optical manipulation has been explored as a method to position individual nanowires as well. This was first demonstrated by Yu *et al.* [7], with CuO wires being held against a surface in line optical tweezers. Agarwal and colleagues [8] showed the trapping, near a surface, of multiple CdS nanowires in dynamic holographic line tweezers, with the possibility of rotating, cutting, and fusing the wires. The first three-dimensional trapping away from the surface was reported by Pauzauskie *et al.* [9], who demonstrated trapping of nanowires, including GaN, ZnO, and Si, along the beam axis of the optical tweezers. Here, use was made of the fact that wires in an optical trapping beam experience forces that tend to align the wires along the optical axis. Limited rotational control, however, was in this case only obtained at the surface, after positioning one end of the wire onto the surface.

The reason all experimental work so far has been limited to manipulation of nanowires near a surface, is because three-dimensional in-plane trapping of high-refractive index wires is frustrated by the large destabilizing scattering force. Particles in a laser beam experience this so-

called scattering force [10] in the propagation direction of the laser light. For a strongly scattering semi-conducting wire in single-beam line tweezers, this force can — depending on the refractive index and thickness of the wire — be too large to be compensated by the so-called gradient force [10]: the particle cannot be trapped in three dimensions.

In this article, we demonstrate counter-propagating dual-beam line tweezers, in which ZnO and silica-coated Si nanowires are stably trapped in three dimensions, away from the surface. The use of two opposing high-numerical aperture objectives supplies the necessary intensity gradient, while the scattering forces from each side counter-act each other [11, 12]. The scanning of the line tweezers with Acousto-Optic Deflectors (AODs) enables full dynamic in-plane orientational control over the nanowires.
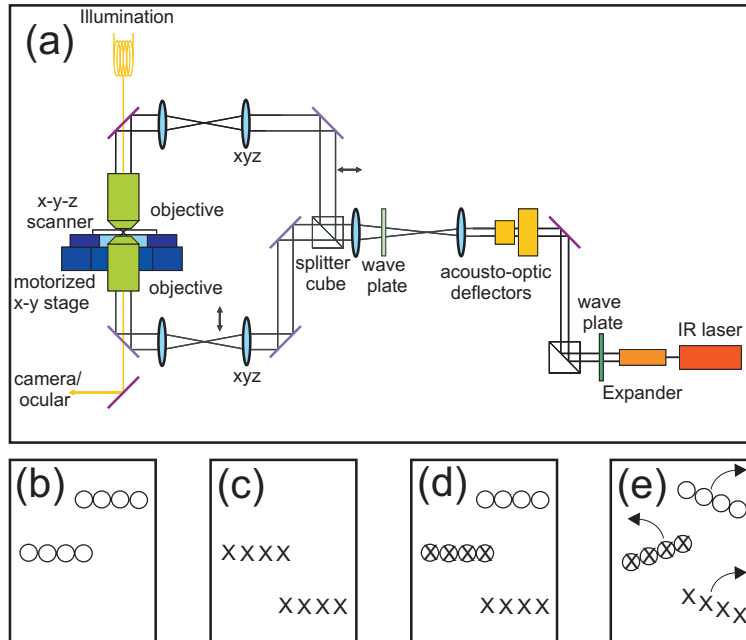

Fig. 1. (a) Schematic of the counter-propagating optical tweezers setup. (b-e) Alignment and rotation of the counter-propagating traps. (b) The inverted beam line trap (○) is positioned left of the center of the frame, with its mirror image at the top right. (c) The upright beam line trap (×) is also positioned left of the center of the frame, with its mirror image at the bottom right. (The mirror symmetry is left-to-right.) In (d) the traps are shown superimposed on each other, forming the counter-propagating traps (⊗). (e) The counter-propagating traps can be moved arbitrarily using the AODs, and are here depicted rotating in an anti-clockwise direction.

2. Experimental methods

2.1. Optical tweezer setup

To allow for counter-propagating beam trapping in our setup (Fig. 1(a)), the condenser of an inverted microscope (Leica, DM IRB) was replaced by a second high-numerical aperture objective (both objectives: Leica, 100×, 1.4 NA, oil immersion). For a more detailed description of the setup, see Ref. [13]. An infra red laser beam (Spectra Physics, Millennia IR, 10 W cw, 1064 nm) was split at a polarizing beam splitter cube, while the rotation of a half-lambda wave plate determined the ratio between the power sent to the lower inverted objective and the power sent

to the upper upright objective. In both beam paths a pair of lenses formed a telescope to provide manual xyz-displacement of the laser focus (all four lenses: $f = 80$ mm). The use of dichroic mirrors (Chroma Technology Corp.) allowed for illumination and imaging in the visible. Before splitting, the laser beam passed through a pair of AODs (IntraAction, DTD-276HB6), with which the xy-displacement of the laser traps inside the sample was controlled, and time-shared [14] line traps were created. The AODs were positioned at a plane conjugate to the back focal planes of the objectives, and the signals to the deflectors were supplied by Direct Digital Synthesizers (DDS; Novatech Instruments Inc., DDS8m). The beam was expanded to fill the back of the objectives. This was done in two steps: before the AODs by a $6\times$ beam expander (Melles Griot), and after the AODs $\sim2\times$ by a pair of lenses ($f = 120$ mm and $f = 250$ mm).

During counter-propagating trapping, the two objectives remained at a fixed distance from each other. To move the traps, the sample cell was moved with respect to the objectives, using motorized actuators (Newport, 850G-LS) mounted on an xy-stage (Rolyn, 750-MS) for long range displacement, in addition to an xyz-piezo stage (PI, $300\times300\times300$ μm^3) for accurate positioning. A digital Charge Coupled Device (CCD) camera (Uniq Vision, UP-600) was used for imaging in brightfield microscopy.

2.2. Counter-propagating line tweezers

Using the AODs, line tweezers were created, which consisted of individual traps spaced ~0.9 μm apart. Due to the configuration of the counter-propagating beam paths, a pattern focused by the upright objective (Fig. 1(b)) is mirrored with respect to that pattern focused by the inverted objective (Fig. 1(c)). To not be limited to symmetric patterns, we scanned both the desired line pattern and its mirror image. Then, inside the sample, we placed the line pattern from the inverted beam opposite the mirror image from the upright beam using the xyz telescope lenses. This way, one line of counter-propagating tweezers (Fig. 1(d)) was created, while the in-plane orientation and length of the line trap could be chosen arbitrarily (Fig. 1(e)). Switching from one pattern to another with differently oriented lines (Fig. 2), enabled full dynamic rotational control over the trapped nanowires.

The alignment in the xyz-direction of the inverted and the upright beams was investigated by looking at the camera image of the trapping beams. After removing the IR filter in front of the camera, the upright beam, as well as the reflection of the inverted beam, were visible when focusing the inverted objective near the glass-medium interface (Fig. 2). Now, the divergence of the two beams was changed (thus moving the z-positions of the foci) until satisfactory focused images appeared for both beams. Then, the line traps were placed on top of each other in the xy-direction.

In this scheme the counter-propagating line tweezers are always accompanied by two single-beam line tweezers; one inverted and one upright. The loss of half of the laser power into these single-beam traps, however, does not pose a problem when using a high-power laser beam. The lines can be placed far away from the counter-propagating line tweezers, as far as the range of the AODs allows (in combination with the $100\times$ objective this is approximately 28×28 μm^2). In the presented experiments, the typical laser power used was 1–2.5 W, corresponding to ~120–300 mW in the counter-propagating line tweezers.

Depending on the length of the nanowires, we used lines varying from approximately 3.6 to $11\,\mu$m. The two lines of a pattern were addressed one after the other, for each line starting at the center point, going, alternatingly left and right, outwards. DDSs provided the signals to the AODs, and a LabVIEW program was used to create and switch between different patterns of traps. Addressing a whole pattern was done on a time scale of <1 ms; fast enough compared to the Brownian motion of a trapped nanowire in the tweezers.

The proposed method of creating counter-propagating traps using a mirror image of the pat-
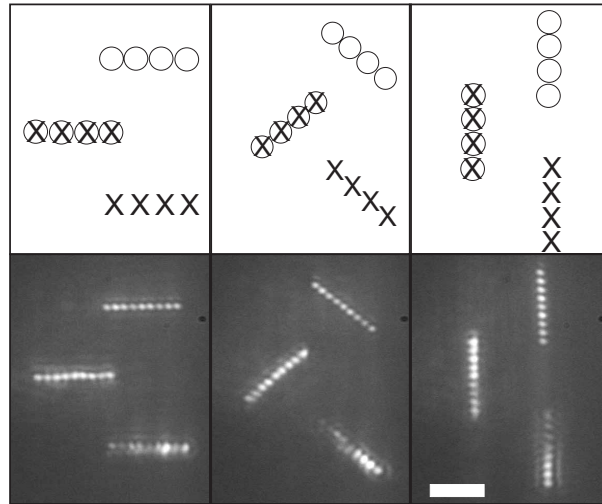
Fig. 2. A sequence of microscopy images of the counter-propagating traps rotating through 90° in 10° steps (not all steps shown). The counter-propagating line trap (on the left), which consists of 9 individual traps, rotates in an anti-clockwise direction, with the mirror images of the line trap rotating in a clockwise direction (3.4 MB movie). The upright traps are directly imaged, while the inverted traps are visible due to light reflected at the glass-medium interface in the sample. The top images show the schematic representation of the rotating counter-propagating ($\otimes$) line trap (with four traps per line shown). ($\bigcirc$) indicates inverted traps and ($\times$) indicates upright traps. Scale bar is 5μm.

tern, ensures great flexibility. The traps can be placed at arbitrary positions, not only to create a counter-propagating line trap as is here demonstrated, but to create any — dynamic — configuration of counter-propagated traps. In addition, the mirror image can be scaled in size, to compensate for scaling differences between upright and inverted beam (whether due to the use of different magnification objectives, or to differences introduced elsewhere). Moreover, the power ratio between inverted and upright beam can be set for each individual trap. By changing the amplitude of the signal to the AODs, or the time the signal lingers at certain frequencies, the power ratio between traps can be adjusted. Now, because for each counter-propagating trap the inverted and the upright beam are addressed independently, the ratio of power for each trap can be controlled. This can be used to compensate for position dependence of laser power (e.g. due to differences in AOD efficiency), and also to move a trapped particle (slightly) along the beam axis, or, in the case of nanowires, to tilt a wire out of the focal plane.

2.3. Sample preparation

ZnO nanowires (n =1.9 at 1064 nm, 50-100 nm in diameter) were synthesized using a Vapour-Liquid-Solid technique [15, 16]. The nanowires were removed from their Si\SiO$_2$ substrate and suspended in ethanol by sonicating for a few seconds. The synthesis of the 200-nm-thick Si nanowires (n =3.6) , which were coated with a 50-nm-thick layer of silica (n =1.45), is described elsewhere [17]. Sample cells (approximately 20 to 40 μm thick) were prepared from a 22-mm-diameter round cover slip (base) and an 18-mm-diameter round cover slip (top) with about $5 - 10 \mu$L of a dilute dispersion of nanowires between. To prevent evaporation of the ethanol, the cell was sealed with candle wax. In some cases we deposited silica particles ($\sim$ 1.2 μm diameter) on the top cover slip by depositing a few drops of a dilute dispersion of silica particles in ethanol on the cover slip and allowing the ethanol to evaporate. We then adsorbed a
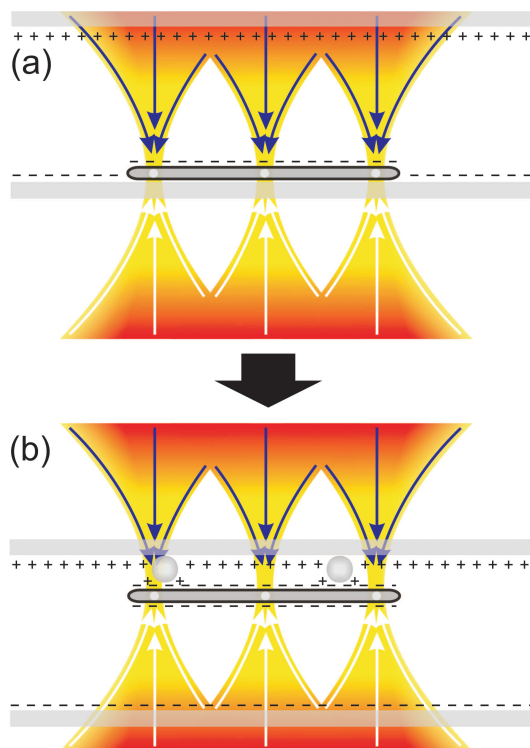
Fig. 3. A sketch showing a nanowire trapped in counter-propagating traps. (a) The nanowire is trapped at the bottom of the sample cell. Because it has the same sign of surface charge (negative) as the cell wall, it does not stick to the wall and can be lifted from the bottom of the cell (by lowering the piezo stage) and moved in the xy plane (by moving the motorized actuators) or even rotated (see Figs. 2 and 4). (b) The top surface of the cell and the silica particles deposited onto it, have been coated with PAH to give them a positive charge. When pressed against the top surface the nanowire will stick through electrostatic interactions. Here the nanowire is shown forming a bridge between two spheres (see Fig. 8).

layer of the positively charged polyelectrolyte poly(allylamine hydrochloride) (PAH) on to the surface. The PAH was adsorbed from an aqueous solution at a concentration of $12\,\mathrm{mg\ mL^{-1}}$ (0.5 M NaCl) by immersing 18-mm-diameter cover slips in the solution and stirring. After 2 hours they were removed from the solution and placed in a bath filled with deionized water (Labconco WaterPro PS) which was stirred for 24 to 36 hours. During this period the water was replaced three times. This extended period of washing ensured that there was little or no PAH free in solution.

Because the base cover slips of the sample cells were negatively charged, as were the nanowires, the wires could reside at the bottom without getting stuck (Fig. 3(a)). Here, they could be trapped, lifted off of the bottom, and manipulated using the optical tweezers. The PAH coating of the top surface provided an electrostatic attraction between this surface of the cell and the negatively charged nanowires (similar to the procedure we developed for spheres [18]). As a result, when brought together, the nanowires would stick to the PAH-coated top cover slip or to the coated silica particles (schematically depicted in Fig. 3(b)).
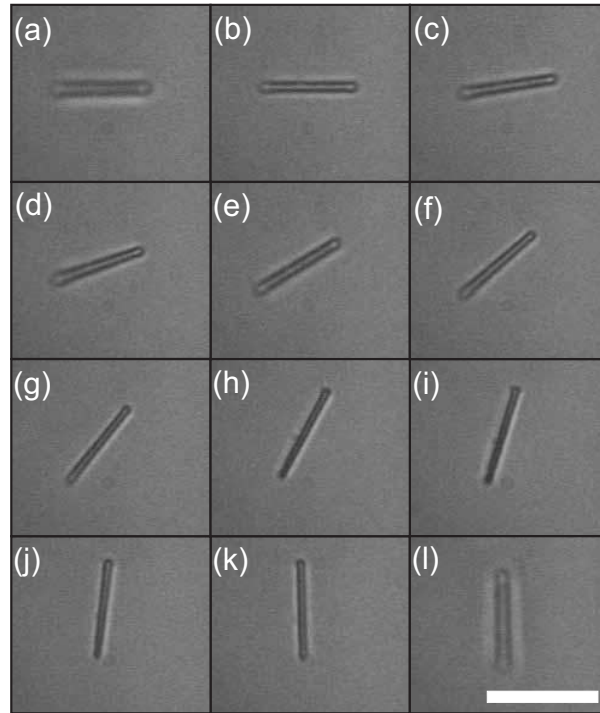
Fig. 4. A 6-μm-long ZnO nanowire trapped in a counter-propagating line trap (2.6 MB movie). (a) The nanowire is caught in the counter-propagating trap at the bottom of the $\sim 20\,\mu$m deep cell. (b) Three-dimensionally trapped, the nanowire is lifted $\sim 10\,\mu$m off the bottom of the cell. (c-k) The nanowire is rotated through 90° in steps of 10° (see also Fig. 1). (l) Whilst still trapped the nanowire is lowered back to the bottom of the cell, where it is pushed out of focus by the glass. Scale bar is $7\,\mu$m.

3.   Experimental results and discussion

Using single-beam line tweezers, the ZnO and silica-coated Si nanowires could be trapped against the surface. But three-dimensional trapping in the plane perpendicular to the beam-axis was not possible in single-beam line tweezers; the nanowires were expelled from the laser focus (not shown).

In counter-propagating line tweezers, however, we were able to stably trap these high-refractive index nanowires, translate them in all three dimensions, and rotate them in the plane perpendicular to the beam axis. In Fig. 4(a), a 6-μm-long ZnO wire is trapped at the bottom of a $\sim 20\,\mu$m deep sample cell. By moving the piezo stage down, the nanowire is then lifted $\sim 10\,\mu$m off of the bottom (Fig. 4(b)), and rotated through 90° in steps of 10° (Fig. 4(c–k)). During the rotation steps, the trapping plane of the wire moved slightly in the z-direction, along the beam-axis. In Fig. 4(l) the ZnO nanowire is lowered again, and pressed against the bottom of the cell, causing the nanowire to move out of focus. Although the nanowires were rotated in steps of 10°, it is possible to rotate the nanowires in smaller steps by simply generating more intermediate patterns for the AODs.

The change in z-position of the trapping plane with respect to the focal plane of the imaging objective for different angles of the line tweezers, was observed for all trapped ZnO nanowires. During stable counter-propagating trapping, the focal planes of the two opposing objectives did not exactly coincide. The polarization directions of the two trapping beams were perpendicular
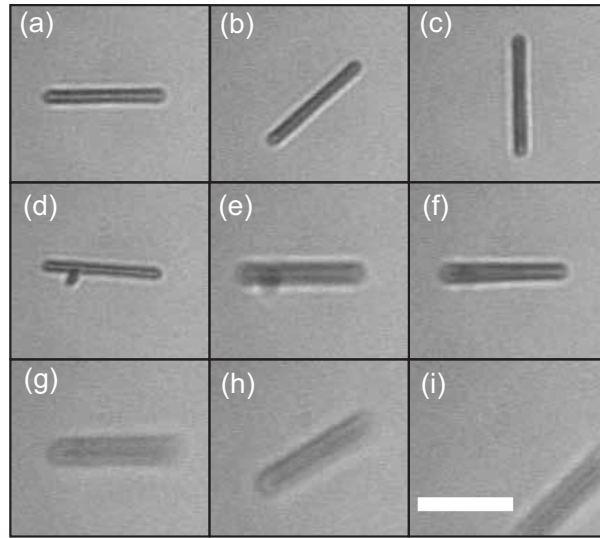
Fig. 5. (a–d) A Si nanowire is pressed against the bottom coverslip and rotated through 90° and back again, with the majority of the laser power through the upright trap. (e) The trap is raised from the bottom cover slip - the nanowire is seen to go out of focus. The balance of the traps is readjusted between e and f and the nanowire jumps (almost) back into focus. (g–i) The nanowire is raised to the top of the cell (about 10 microns) and is pressed against the top cover slip. As the nanowire is rotated it pops out of the trap (i). Scale bar is $5\,\mu$m.

with respect to each other, and the trapped nanowires tended to move towards the focal plane of the beam for which the polarization was parallel to the orientation of the line trap. This is in accordance with the alignment of an elongated particle of its long axis parallel to the polarization direction of the trapping light [19, 20], and with the stiffer trapping of a spherical particle in the direction perpendicular to the polarization direction [21]. (The polarization of the inverted beam is oriented left-to-right in the camera image, while the polarization of the upright beam is top-to-bottom.)

Figure 5 shows a silica-coated Si nanowire trapped in counter-propagating line tweezers. Due to their higher index of refraction and relatively large thickness, the Si nanowires were harder to stably trap as compared to the ZnO nanowires, and alignment of the line tweezers was more precarious. While ZnO nanowires positioned $> 15\,\mu$m away from the surface could be trapped in counter-propagating line tweezers simply by positioning the line tweezers in the vicinity of the wire (not shown), we were only able to trap the Si nanowires by starting at the surface. In Fig. 5(a–d), a Si nanowire, approximately $6\,\mu$m in length, was pressed against the bottom surface and rotated over 90° and back again. The majority of the laser power was through the upright trap. Then, the piezo stage was moved down, and the nanowire moved down with it (Fig. 5(e)). By adjusting the ratio of laser power by manually rotating the half-wave plate, and thus having more power from the inverted trap, the wire was lifted off of the bottom and three-dimensionally trapped. At the top surface the nanowire was rotated again (Fig. 5(g–h)), after which it was expelled from the line tweezers (Fig. 5(i)), possibly due to a slight change in power ratio or in alignment of the two line tweezers for the different orientation. The silica-coated Si nanowires we used were relatively thick, and thinner Si wires are expected to be more easily stably trapped in counter-propagating traps, making the alignment and power ratio setting less critical. In this experiment we changed the ratio of laser power by manually rotating the half-wave plate before the polarizing beam splitter cube. However, the independence of our

counter-propagating line tweezers makes it also possible to tune the power of individual traps using the AODs, as discussed earlier.

The 3D trapping and in-plane rotation of semiconducting nanowires can be applied to pattern surfaces and build larger structures. Here, we demonstate the flexibility of our trapping method by positioning the ends of multiple nanowires on islands of silica particles (schematicly depicted in Fig. 3(b)). Due to the evaporation method used to deposit the silica particles, the islands were randomly distributed over the surface, and wires suitable for the location had to be selected. In dilute dispersions, selected wires of the desired length sometimes were transported over distances $> 1\,\text{mm}$, with speeds of typically $4\,\mu\text{m/s}$, making it possible to interactively avoid other nanowires on the way. When moving in the direction along the nanowire, the trapped nanowires more easily slide out of the trap; therefore, an orientation perpendicular to the moving direction was preferred. After arriving at the location of the structure, we lowered the sample to make the position of the silica particles visible. Then, by lowering the sample cell further, a trapped nanowire could be stuck with its ends onto the PAH-coated islands of silica particles.
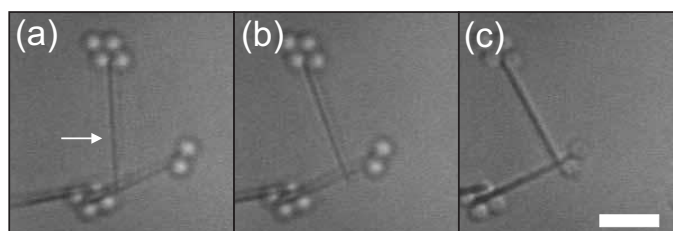

Fig. 6. (a) A ZnO nanowire stuck at one end to previously deposited poly(allylamine hydrochloride) (PAH)-coated silica particles (diameter $\sim 1.2\,\mu\text{m}$). (b) The other end is resting loosely upon a second nanowire that is bridging two islands of silica particles. By trapping the free end of the nanowire in an individual counter-propagating trap it was possible to drag the nanowire until it formed a right angle with the second nanowire (c). Turning up the laser power on the inverted beam trap resulted in the free end of the nanowire sticking to the bridging nanowire. The wire did not move after the laser was turned off. (Short version movie is 2.5 MB and long version movie is 13 MB.) Scale bar is $5\,\mu\text{m}$.
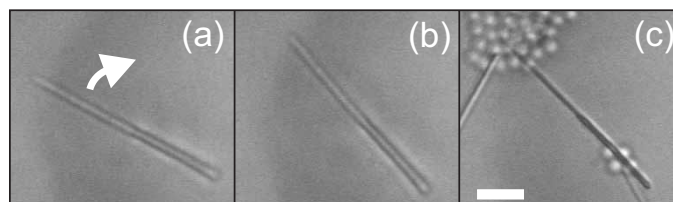

Fig. 7. This sequence of images shows a ZnO nanowire first being rotated in a clockwise direction in a line trap. The wire was positioned under the correct angle, to then be lifted to the top cover slip of the cell where the negatively charged nanowire was stuck to the positively charged surface of silica particles, bridging two separate islands of particles. (Short version movie is 1.3 MB and long version movie is 14 MB.) Scale bar is $5\,\mu\text{m}$.

Figure 6 shows this sticking of a ZnO nanowire in two steps. In this sample, several ZnO nanowires had already been positioned. First, one end of the trapped nanowire (indicated by the arrow in Fig. 6(a)) was placed on a group of four silica particles, at which point it could still rotate. The other end rested upon a second wire, but was not attached to it. In Fig. 6(b) we

employed an individual counter-propagating trap to move this loose end to the right, thereby changing the angle of the wire until it made a right angle with the second nanowire (Fig. 6(c)). Then, by turning up the laser power from the inverted beam trap, the wire was fixed in this position.

A simpler method is to position the nanowire at the correct angle before sticking it. This is shown in Fig. 7. Here we see a 20-μm-long nanowire trapped in counter-propagating tweezers (Fig. 7(a)), being rotated in a clockwise direction (Fig. 7(b)), and then placed onto silica particles, connecting two islands and thereby finishing a larger structure which is shown in Fig. 8. After 24hrs, this structure, consisting of seven islands of PAH-coated silica particles bridged by seven ZnO nanowires, was still intact.
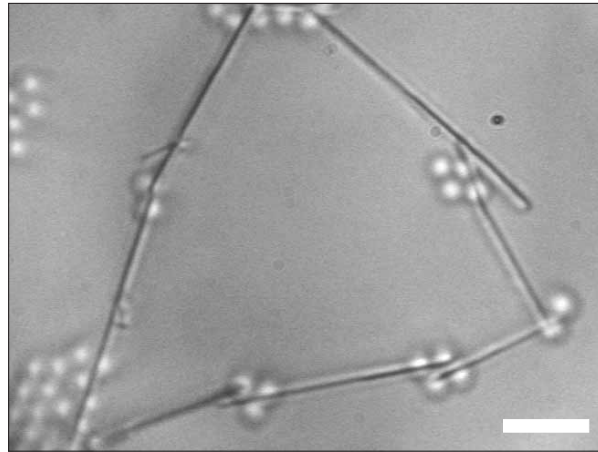

Fig. 8. The final structure constructed by bridging PAH-coated silica particles with ZnO nanowires, imaged in brightfield microscopy. Scale bar is 7 μm.

4. Conclusions

ZnO nanowires were trapped in counter-propagating line tweezers, and lifted 10 μm off of the bottom of the sample cell. Although not shown here, lifting the ZnO wires from bottom to top in a >60 μm thick sample was readily achieved. We showed full rotational control over the nanowires in the plane perpendicular to the beam axes. In addition, we showed the 3D trapping of silica-coated Si nanowires. The trapping of these high-refractive index nanowires (both ZnO and Si) in the plane perpendicular to the beam axis away from the surface, was not possible with single-beam line tweezers — in the axial direction no sufficient gradient force could be obtained to balance the destabilizing scattering force. To the best of our knowledge, stable trapping of high-refractive index nanowires parallel to but away from the surface has not been shown before.

Scanning the laser using the AODs enabled us to produce counter-propagating line tweezers of a precisely controlled length. By simply adding or removing traps from the line scanned, we were able to alter the length of the line trap at will. This gave a significant improvement on the ability to trap the nanowires along the line of the trap, compared to the method of simply spreading the laser spot as reported by Yu *et al.* [7].

Due to the independence between the inverted beam pattern and the upright beam pattern, differences in scaling factor between the two beam paths can be compensated for. In addition, the power ratio of each individual counter-propagating trap can be controlled. Although we did

not investigate this further, this feature can be used to tilt trapped nanowires with respect to the focal plane of the objectives.

As a demonstration, ZnO nanowires were lifted from the bottom surface, translated in the sample cell, and placed onto the top surface, or, alternatively, positioned on top of silica spheres. By only creating opposite charged walls at the top surface of the sample cell, freely diffusing wires could reside at the bottom of the cell. These wires could then be selected and transferred to another location within the cell, before being stuck to the top surface. This way, configurations and structures of nanowires on the surface can be made permanent for use in, for example, photoluminescence experiments. By trapping the nanowires perpendicular to the beam direction, we were able to rotate and position the nanowire prior to sticking any part of the nanowire to the surface. This gave greater control and therefore precision over where the length of the wire was placed compared to the 'stick and drag' method [9]. The ability to place nanowires at a surface in precisely controlled positions will be critical in the production of nanoelectronic and nanophotonic devices.

Acknowledgements